Tight-binding calculations of the optical properties of HgTe nanocrystals

Guy Allan and Christophe Delerue*

Institut d'Electronique, de Microélectronique et de Nanotechnologie - Département Institut Supérieur d'Electronique et du Numérique, UMR CNRS 8520, Lille, France

(Received 27 June 2012; published 23 October 2012)

We propose a tight-binding model of HgTe which gives an accurate band structure in a wide energy range compared to recent *ab initio* calculations. The inverted band structure near the Fermi level and its temperature dependence are also very well described. Using this parametrization, we study the effects of the quantum confinement on the electronic structure of HgTe quantum dot nanocrystals. We calculate the optical absorption spectra of quantum dots with various shapes and diameters up to 10 nm. We show, using a configuration interaction approach, that excitonic effects are negligible in this range of sizes. Our predictions for the size dependence of the energy gap and for the optical spectra are consistent with recent experimental data.

DOI: 10.1103/PhysRevB.86.165437 PACS number(s): 78.67.Bf

I. INTRODUCTION

Colloidal quantum dots (QDs) with optical gap in the infrared or in the near infrared are promising building blocks for a wide number of optoelectronics applications, in particular, for the production of cheap photovoltaic thin films or infrared detectors.[1,2] In this context, lead chalcogenide QDs have been the most studied,[2–4] but HgTe presently receives growing interest because its zero band gap in the bulk enables complete tunability from the infrared to the near infrared in QDs thanks to the quantum confinement.[5–15] For example, photoresponse of HgTe QD films in the atmospheric transparency window between 3 and 5 μm has been recently demonstrated.[13]

It is thus particularly important to perform theoretical modeling of HgTe QDs (Refs. 14 and 16) in order to predict their optical properties and to interpret the experiments. The difficulty in this task comes from the peculiar electronic structure of HgTe near the Γ point. HgTe has an inverted band structure[17] (the *s*-like Γ_6 band lies below the *p*-like Γ_8 band); the conduction-band effective mass is very light ($\approx 0.01 m_0$) but already 50 meV from the band edges the dispersion of the electron and light-hole bands is no longer parabolic.[18] In addition, the $\Gamma_6 - \Gamma_8$ gap energy strongly varies with temperature.[19] Modeling the optical properties in the (near)-infrared thus requires a good description of bands near the Γ point, but even state-of-the-art *ab initio* methods have difficulties in this task.[20–23] For this reason, $\mathbf{k}\cdot\mathbf{p}$ is still considered a theoretical method of choice to study the electronic structure of HgTe nanostructures because it is specifically designed to describe the bands in this important region.[18,24]

In this paper, we present a tight-binding (TB) model of HgTe which gives an excellent band structure in a wide energy range compared to Hedin's GW calculations[21] and, at the same time, a very accurate dispersion near the Fermi level and the Γ point compared to a $\mathbf{k}\cdot\mathbf{p}$ approach.[18] With these parameters we calculate the electronic structure and the optical absorption spectra of HgTe QDs. Calculations based on a configuration interaction (CI) technique demonstrate that excitonic effects can be neglected for QD diameters below at least 10 nm. We show that recent experimental results on HgTe QDs[14,15] are correctly described taking into account the uncertainty on the QD shape. The TB model can be used to study many other problems related to HgTe nanostructures. For example, HgTe is also widely investigated as a topological insulator when a gap is open by the confinement.[25,26]

II. METHODOLOGY

A. TB electronic structure

The electronic structure of HgTe is calculated in TB as described in the Appendix. The TB Hamiltonian matrix is written in a basis of atomic orbitals ($sp^3d^5s^*$) as a function of a small number of parameters (Table I in the Appendix) which, in the present case, are obtained by fitting on two reference band structures: (1) close to Fermi level at $\mathbf{k} = 0$, on the $\mathbf{k}\cdot\mathbf{p}$ band structure of Ref. 18; (2) elsewhere in the Brillouin zone, on the band structure of Ref. 21 obtained using a quasiparticle self-consistent GW approximation in a hybrid scheme (20% LDA and 80% GW). The good agreement with these two reference band structures is demonstrated in Figs. 1 and 2. It is important to point out that the $\mathbf{k}\cdot\mathbf{p}$ Hamiltonian gives a very good description of the infrared absorption in bulk HgTe (Ref. 18) and explains rather well the optical properties of HgTe QDs.[14]

Since the band structure at Γ strongly depends on the temperature, we have determined TB parameters for 0 and 300 K. With these values, we obtain a $\Gamma_6 - \Gamma_8$ gap energy of -0.31 eV (–0.14 eV) at 0 K (300 K), in agreement with the experimental value of -0.30 eV (–0.12 eV).[19] The spin-orbit splitting $E_{\Gamma_8} - E_{\Gamma_7}$ is equal to 1.06 eV, also close to reported values.[27] An accurate band structure as shown in Figs. 1 and 2 is a prerequisite to obtain good results for QDs with a large variety of sizes and shapes.[28] It cannot be obtained with the same accuracy using first-nearest-neighbor sp^3s^* TB models.[29–32]

The *s*-like projection of the wave functions is shown in Fig. 3 for the main bands near the Fermi level. The light-hole band (Γ_6) has a pure *s* character at $\mathbf{k} = 0$, but the *s* weight decreases very quickly when $\mathbf{k}$ moves away from Γ. On the contrary, the electron band has some *s* character everywhere except at Γ. Very similar behavior of the *s* weight with $\mathbf{k}$ is obtained using hybrid density functional theory.[22]

B. Excitonic states and configuration interaction

In order to evaluate the importance of excitonic effects in the optical spectra of QDs, we have calculated the excitonic states

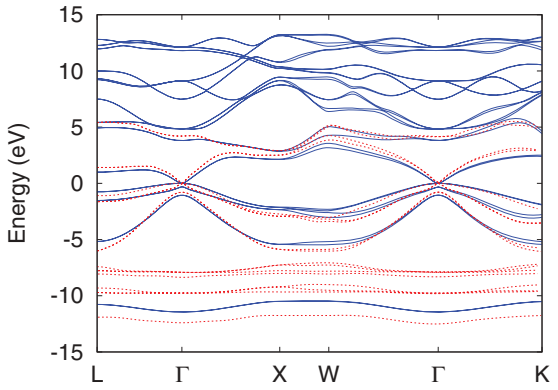

FIG. 1. (Color online) Band structure of HgTe at 0 K calculated in TB. The red dots indicate the values obtained in Ref. 21 using a hybrid GW approach. The zero of energy corresponds to the top of the valence band.

$|\Psi^i_{\rm exc}\rangle$ using a CI method.[28,33,34] Schematically, following the well-known GW plus Bethe-Salpeter approach for excitons,[35] the formation of the exciton can be seen as the result of two processes: the injections of independent electron and hole in the QD (GW) and their coupling by the electron-hole interaction (Bethe-Salpeter). Therefore, in a first step, we calculate the self-energy corrections to the TB energies induced by the injection of the separate electron and hole in the QD. As shown in Ref. 36, these self-energy corrections mainly come from the dielectric polarization of the QD; they are given by the resultant interaction between the injected carrier and the polarization charges. They also correspond to the Coulomb-hole term of the static COHSEX (Coulomb hole plus screened exchange) approximation.[35,36] As usual in GW, the self-energy corrections are assumed to be diagonal in the basis of the electron and hole states. This approximation is particularly justified in the strong confinement regime because the self-energy couplings are small compared to the confinement energies. In the second step, the electron-hole interaction is introduced, leading to a two-particle problem (Bethe-Salpeter). The excitonic Hamiltonian is defined in the basis of Slater determinants $|\psi_{vc}\rangle$ built from the TB

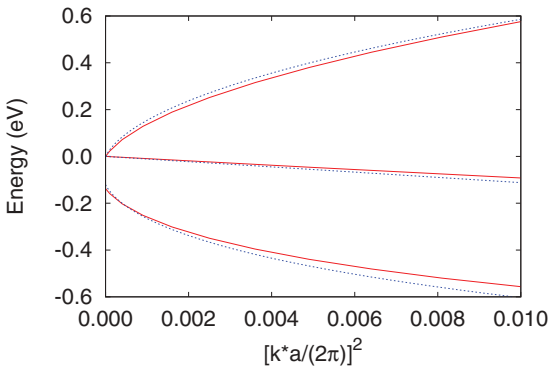

FIG. 2. (Color online) Band structure of HgTe at 300 K for $\mathbf{k} \parallel [100]$ close to the Γ point. The energies are plotted versus $[ka/(2\pi)]^2$, where $k = |\mathbf{k}|$ and a is the lattice parameter. The bands calculated in TB (red solid lines) are compared with those obtained from the $\mathbf{k}\cdot\mathbf{p}$ approach of Ref. 18 (blue dotted lines).

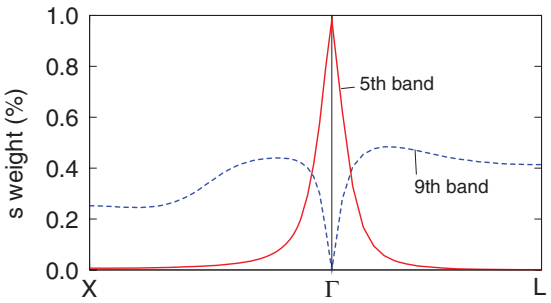

FIG. 3. (Color online) Weight of the projection of the wave function on the s orbitals as a function of the wave vector $\mathbf{k}$ along ΓX and ΓL (calculated at 0 K). The results are shown for the fifth (Γ_6, light-hole) and ninth (Γ_8, electron) bands (the first band being the lowest one in Fig. 1). The s weight is zero for the seventh band (Γ_8, heavy hole). Very similar results are obtained at 300 K.

single-particle states. With respect to the ground state $|0\rangle$ corresponding to filled valence states and empty conduction states, $|\psi_{vc}\rangle$ represents the system with an electron-hole pair in which the valence state v has been replaced by the conduction state c. The matrix elements of the excitonic Hamiltonian in this basis are given by

$$\begin{aligned}&\langle\psi_{vc}|H|\psi_{v'c'}\rangle\\&\quad=([\varepsilon_c+\Sigma_c]-[\varepsilon_v+\Sigma_v])\delta_{cc'}\delta_{vv'}\\&\qquad-\int c^*(\mathbf{x}_1)v^*(\mathbf{x}_2)V_{\rm coul}(\mathbf{r}_1,\mathbf{r}_2)c'(\mathbf{x}_1)v'(\mathbf{x}_2)d\mathbf{x}_1d\mathbf{x}_2\\&\qquad+\int c^*(\mathbf{x}_1)v^*(\mathbf{x}_2)V_{\rm coul}(\mathbf{r}_1,\mathbf{r}_2)v'(\mathbf{x}_1)c'(\mathbf{x}_2)d\mathbf{x}_1d\mathbf{x}_2,\end{aligned}\quad(1)$$

where $\mathbf{x}_1$ stands for $(\mathbf{r}_1,\xi_1)$, in which ξ_1 represents the spin variable of the particle 1. The second line in Eq. (1) corresponds to the screened Coulomb interaction between the electron and the hole, and the third line contains the exchange term. $V_{\rm coul}(\mathbf{r}_1,\mathbf{r}_2)$ describes the energy of a charge $+e$ at $\mathbf{r}_1$ in the screened potential of a charge $+e$ at $\mathbf{r}_2$:

$$V_{\rm coul}(\mathbf{r}_1,\mathbf{r}_2)=\int\epsilon^{-1}(\mathbf{r}_1,\mathbf{r})\frac{e^2}{|\mathbf{r}-\mathbf{r}_2|}d\mathbf{r},\quad(2)$$

in which $\epsilon^{-1}(\mathbf{r}_1,\mathbf{r})$ is the generalized dielectric constant (here taken in the static limit). We have considered a screened electron-hole exchange term in the third line of Eq. (1) instead of a bare one as in the original derivation of the Bethe-Salpeter equation,[35] because it seems more appropriate when a finite set of electron-hole states is used.[28,37] In any case, this exchange term has a negligible influence on the spectra shown in this paper, as it only affects the fine structure of the exciton.

As discussed above, the term Σ_c (Σ_v) in Eq. (1) represents the self-energy of the electron (hole) coming from its interaction with the polarization charges induced at the surface of the QD by its own presence[28,36] (the Coulomb hole term of the COHSEX approximation),

$$\Sigma_c=\frac{1}{2}\int|c(\mathbf{r}_1)|^2\lim_{\mathbf{r}_2\to\mathbf{r}_1}\left(V_{\rm coul}(\mathbf{r}_1,\mathbf{r}_2)-\frac{e^2}{\epsilon_{\rm in}|\mathbf{r}_1-\mathbf{r}_2|}\right)d\mathbf{r}_1,\quad(3)$$

where $\epsilon_{\rm in}$ is the dielectric constant of the material at the position $\mathbf{r}_1$. Σ_v is defined similarly. $V_{\rm coul}$, the Coulomb and exchange

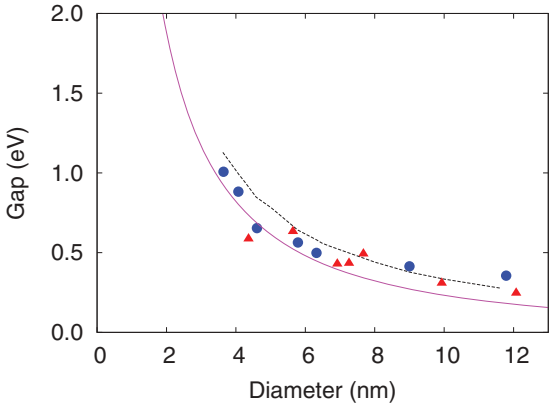

FIG. 4. (Color online) Energy gap of spherical HgTe QDs (300 K) versus diameter (magenta solid line) compared to the experimental data of Ref. 14 (red triangles) and Ref. 8 (blue disks). The black dotted line represents the energy of the second peak in the calculated absorption spectrum.

terms, and the self-energies can be accurately calculated using classical electrostatics for QDs with diameter above ≈2 nm.[28,36,38] In the case of a spherical QD, we simply describe the system as a dielectric sphere of dielectric constant ϵ_{in} in a medium of dielectric constant ϵ_{out}. We use $\epsilon_{\text{in}} = 13$ for HgTe (Ref. 27) and $\epsilon_{\text{out}} = 2.25$ for the solvent employed in Ref. 14.

C. Calculation of the optical spectra

The optical cross section of a single QD is calculated as[28,39]

$$\sigma(\hbar\omega) = \frac{4\pi^2 e^2 F^2}{cn} \sum_i \omega_i \left| \langle 0| \sum_n \mathbf{e}.\mathbf{r}_n |\Psi^i_{\text{exc}}\rangle \right|^2 L(\hbar\omega - \hbar\omega_i), \tag{4}$$

where $\hbar\omega$ is the photon energy, $\hbar\omega_i$ is the energy of the excitonic state $|\Psi^i_{\text{exc}}\rangle$ (eigenvector of the Hamiltonian given in Eq. (1), $\mathbf{e}$ is the polarization vector, $n \approx \sqrt{\epsilon_{\text{out}}}$, and $F = 3\epsilon_{\text{out}}/(\epsilon_{\text{in}} + 2\epsilon_{\text{out}})$ is the local-field factor.[28] $\langle 0| \sum_n \mathbf{e}.\mathbf{r}_n |\Psi^i_{\text{exc}}\rangle$ is the dipolar matrix element in which $\mathbf{r}_n$ is the position of the electron n. The function L in Eq. (4) is a Gaussian, $L(x) = \exp[-x^2/(2\sigma^2)]/(\sigma\sqrt{2\pi})$, which describes the broadening of the optical transitions. All the results presented in this work are obtained with $\sigma = 35$ meV.

In the single-particle approximation, the sum over the exciton states in Eq. (4) becomes a sum over electron-hole pair states $|\psi_{vc}\rangle$ and the dipolar matrix element is just replaced by $\langle c|\mathbf{e}.\mathbf{r}|v\rangle$.

III. RESULTS AND DISCUSSION

A. Electronic structure and energy gap of HgTe QDs

The energy gap of spherical QDs is plotted versus size in Fig. 4. It varies in ways such as $1/(0.02126 \times d^2 + 0.21562 \times d + 0.01684)$ (in electronvolts), with d the diameter in nanometers. As already shown for other semiconductor materials,[28,40] the gap of QDs with cubic, tetrahedral, or octahedral shape is very close to the gap of spherical QDs with the same volume. Therefore the same expression of the gap can be used for these shapes if we define d as the diameter of the equivalent sphere. Experimentally, various shapes including spheres and tetrahedra seem to be obtained after colloidal synthesis,[8,11,14] but triangles are often observed by transmission electron microscopy. In spite of the uncertainty on the shape, the agreement between the theoretical gap and the measured absorption edge[8,14] is good, even if the theory seems to be too low compared to experiments at large size. An explanation of this difference is discussed below.

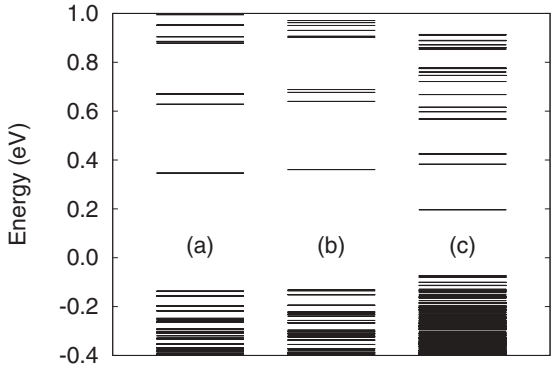

FIG. 5. Calculated energy levels in HgTe QDs at 300 K [(a) sphere, $d = 5.98$ nm; (b) octahedron, $d = 5.83$ nm; (c) sphere, $d = 8.99$ nm]. The zero of energy corresponds to top of the bulk valence band.

The energy levels of three QDs are depicted in Fig. 5. Spherical and octahedral QDs with almost the same diameter (here ≈6 nm) have similar electronic structure, at least near the energy gap. The density of states is considerably higher in the valence band than in the conduction band.

B. Optical absorption spectra

The optical cross sections predicted for HgTe QDs are shown in Fig. 6. We have found that the excitonic effects are very small for all the QD sizes (d up to 10 nm) that we have investigated. The spectra obtained using CI and single-particle approaches are almost identical, except for a small rigid shift in energy. This result can be understood by a large excitonic

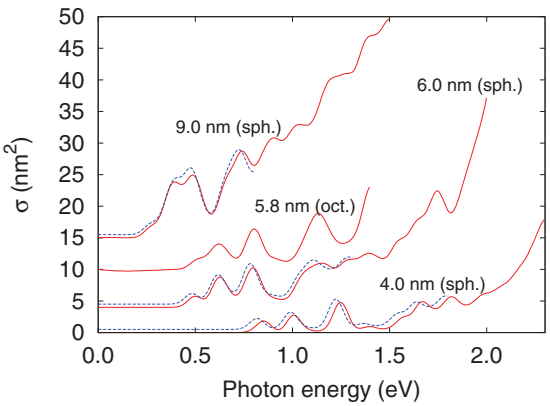

FIG. 6. (Color online) Optical cross section of spherical (sph.) or octahedral (oct.) QDs calculated in TB using the single-particle approximation (red solid lines) or the CI approach including excitonic effects (blue dotted lines). The diameter of the QDs is indicated in the figure. The baseline of each curve is shifted vertically for clarity.

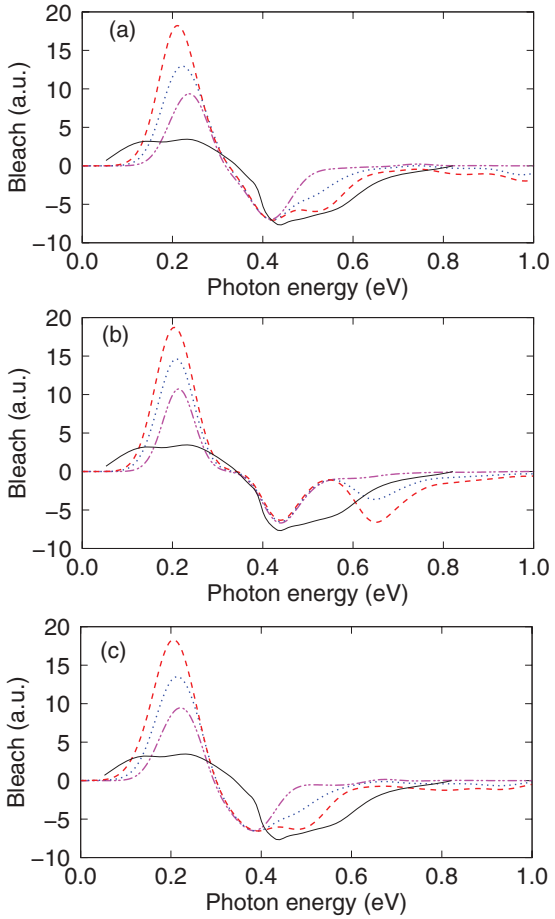

FIG. 7. (Color online) Spectra calculated as the difference in the optical absorption between QDs charged with n electrons and neutral QDs. (Dashed red line: $n = 6$. Blue dotted line: $n = 4$. Magenta dashed-dotted line: $n = 2$.) The QDs have spherical (a), tetrahedral (b), or octahedral (c) shape. Black solid line: experimental difference spectrum (Ref. 15) for electrochemical potential of -1.2 V. Effective diameter of the HgTe QDs: 8 nm. Temperature: 210 K.

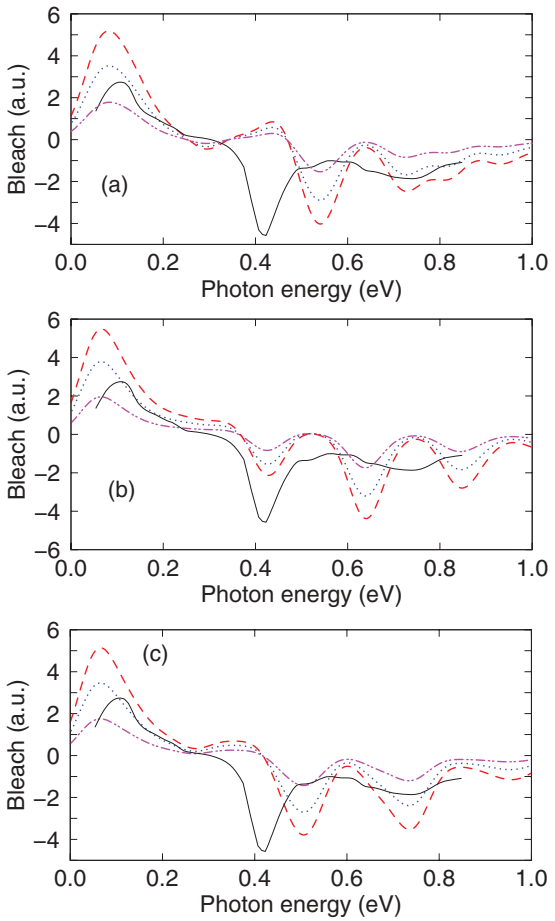

FIG. 8. (Color online) Same as Fig. 7 but for QDs charged with holes. Black solid line: experimental difference spectrum (Ref. 15) for electrochemical potential of $+1.0$ V.

Bohr radius induced by the small electron effective mass. By comparison, the excitonic effects calculated using the same methods are much more pronounced in the case of CdSe or CdTe QDs.[41]

The intensity of the lowest absorption peak in Fig. 6 is clearly decreasing with increasing size, the oscillator strength going to zero in the bulk limit.[20] This behavior is obtained for QDs with spherical, cubic, tetrahedral, and octahedral shapes. For increasing diameters above 6 nm, it is reasonable to consider that the measured absorption edge coincides progressively with our second absorption peak. Figure 4 shows that the position of this second peak agrees very well with the experimental absorption edge for the largest sizes.

C. Infrared absorption of charged QDs

It was recently shown that films of HgTe QDs can be charged with electrons or holes by electrochemistry.[15] Infrared spectroscopy of the charged QDs reveals interband bleach and intraband absorption. A difference spectrum reproduced from Ref. 15 is shown in Fig. 7. It was measured on QDs with rather angular shapes and with diameter estimated around 8 nm. It corresponds to the difference between the infrared absorption spectra taken at -1.2 and 0 V. In that case, it describes the variation in absorption induced by the charging of the QDs with electrons. In order to simulate the experiments, we calculate the optical cross section of charged and neutral QDs, and we compute the difference. In the case of charged QDs, we consider the thermal distribution of the electrons (holes) in the conduction (valence) band since the experiments were performed at 210 K. The electronic structure is also calculated at this temperature.

The spectra obtained for QDs charged with $n = 2$, 4, or 6 electrons are shown in Fig. 7. Those predicted for $n = 6$ agree rather well with experiments, in particular for spherical and octahedral QDs. The evolution with n also qualitatively explains the voltage dependence of the experimental spectra.[15] But the double positive peak measured between 0.1 and 0.3 V is never reproduced by the calculations, even if we predict that the peak broadens when electrons are added to the QDs. We confirm that the double structure cannot be understood if we consider spherical QDs,[15] even if we consider tetrahedral or octahedral QDs. More anisotropic shapes are certainly needed to explain the experimental results, which is compatible with structural characterizations of the QDs.[15]

We have performed a similar analysis in the case of QDs charged with holes (Fig. 8). The spectra calculated for the same QDs qualitatively agree with the experimental ones if we take into account that the position of the negative peaks (interband bleach) varies with the QD shape in a quite sensitive manner. The results obtained for 8-nm QDs are thus consistent with the experimental observations, the octahedral shape giving the best compromise if we consider Figs. 7 and 8 together.

IV. CONCLUSION

In conclusion, we show that a $sp^3d^5s^*$ tight-binding model can reproduce accurately the band structure of HgTe compared to state-of-the-art *ab initio* calculations. The description of the temperature-dependent inverted band structure in the vicinity of the Fermi level is also excellent. We use this model to study the electronic structure and the optical properties of HgTe QDs. Using a configuration interaction approach, we show that excitonic effects are negligible. The variation of the optical gap versus size is in agreement with recent measurements. The shape of the bleach spectra of the QDs after charging by electrons or holes can be explained by the calculations, but important discrepancies between theory and experiments remain, possibly due to uncertainties on the QD shape.[15] The tight-binding parametrization should be also very useful to address many problems which presently receive growing interest, such as topological insulators.[25,26]

APPENDIX: TIGHT-BINDING PARAMETERS FOR HgTe

The electronic structure of HgTe is calculated as described in Ref. 43 for Si and Ref. 44 for III-V materials. In TB,[28,43] the Hamiltonian matrix is written in a basis of atomic orbitals which are assumed to be orthogonal. The matrix elements between two orbitals located on distinct atoms (hopping integrals) are usually restricted to first, second, or third-nearest-neighbor interactions. The Hamiltonian is written as a function of parameters which are adjusted in order to get the best band structure for the bulk semiconductor compared to *ab initio* calculations or experimental results. A minimum basis set of sp^3 atomic orbitals and interactions restricted to first nearest neighbors are not sufficient to describe the conduction band with sufficient accuracy.[28,43,45,46] Therefore we have considered a basis of $sp^3d^5s^*$ (s^* is a second s orbital) orbitals, the hopping terms being restricted to first nearest neighbors.[44,46] Spin-orbit coupling is also included, which requires doubling of the basis set. Following the usual approach in TB,[47] we only consider the intra-atomic terms of the spin-orbit coupling on the p orbitals. Interatomic terms which give rise to the Dresselhaus splitting[48] around Γ due to the lack of inversion symmetry are negligible in this material.[49]

TABLE I. TB parameters [notations of Slater and Koster (Ref. 42)] for HgTe in an orthogonal $sp^3d^5s^*$ model. Δ is the spin-orbit coupling. (a, c) The anion (Te) and the cation (Hg), respectively. E_s(c) is given at 0 and 300 K. Lattice parameter: $a = 6.453$ Å.

Parameters for HgTe (eV)			
E_s(a)	− 10.040161		
E_s(c) (0K)	− 1.502103	E_s(c) (300 K)	− 1.302103
E_p(a)	1.580003	E_p(c)	5.929255
$E_{d_{xy}}$(a)	10.139959	$E_{d_{xy}}$(c)	15.108978
$E_{d_{x^2-y^2}}$(a)	13.145395	$E_{d_{x^2-y^2}}$(c)	15.431086
E_{s^*}(a)	12.611213	E_{s^*}(c)	14.801158
Δ(a)	0.375000	Δ(c)	0.465000
$V_{ss\sigma}$(ac)	− 0.904384	$V_{s^*s^*\sigma}$(ac)	− 1.570513
$V_{ss^*\sigma}$(ac)	0.357261	$V_{ss^*\sigma}$(ca)	− 0.242580
$V_{sp\sigma}$(ac)	1.085069	$V_{sp\sigma}$(ca)	2.014492
$V_{s^*p\sigma}$(ac)	1.175059	$V_{s^*p\sigma}$(ca)	1.405375
$V_{sd\sigma}$(ac)	− 0.525896	$V_{sd\sigma}$(ca)	− 1.067102
$V_{s^*d\sigma}$(ac)	0.485896	$V_{s^*d\sigma}$(ca)	0.696627
$V_{pp\sigma}$(ac)	3.166827	$V_{pp\pi}$(ac)	− 0.945694
$V_{pd\sigma}$(ac)	− 1.789915	$V_{pd\sigma}$(ca)	− 0.653612
$V_{pd\pi}$(ac)	1.406422	$V_{pd\pi}$(ca)	1.657517
$V_{dd\sigma}$(ac)	− 0.529629	$V_{dd\pi}$(ac)	2.424709
$V_{dd\delta}$	− 1.064207		
Parameters for Hg-H and Te-H (eV)			
E_H	2.74638		
$V_{ss\sigma}$	−35.69727	$V_{sp\sigma}$	61.82948

The TB parameters are given in Table I. The terms E represent the on-site matrix elements, E_s being, for example, the s orbital energy in the solid. The zero of energy is taken at the top of the valence band. The energy of the T_2-like d orbitals (xy, yz, zx) is not the same as the energy of E-like ones ($x^2 - y^2$, $3z^2 - r^2$) due to the T_d symmetry in the crystal. Note that these d orbitals are used to describe the conduction bands, not the filled d bands. For example, the rather flat Hg 5d bands between −7 and −10 eV obtained using the GW calculations are not reproduced in TB (Fig. 1) since they are not necessary for our purposes. The terms V in Table I completely define the hopping matrix elements in the two-center approximation as shown by Slater and Koster.[42] For example, $V_{sp\sigma}$(ac) represents the ($sp\sigma$) hopping term between an s orbital on a Te atom and a p orbital on a neighbor Hg atom, the p orbital pointing along the axis between the two atoms, following the notations of Ref. 42. In Table I, two values are given for the on-site s energy of Hg at 0 and 300 K. A linear interpolation can be used for other temperatures.

In the case of HgTe QDs, pseudohydrogen atoms are used to passivate their surface.[28,43] The Hg-H and Te-H parameters are defined in order to push the surface states far from the band edges.

*christophe.delerue@isen.fr

[1] D. V. Talapin, J.-S. Lee, M. V. Kovalenko, and E. V. Shevchenko, Chem. Rev. **110**, 389 (2010).

[2] I. J. Kramer and E. H. Sargent, ACS Nano **5**, 8506 (2011).

[3] C. B. Murray, S. Sun, W. Gaschler, H. Doyle, T. A. Betley, and C. R. Kagan, IBM J. Res. Dev. **45**, 47 (2001).

[4]F. W. Wise, Acc. Chem. Res. **33**, 773 (2000).
[5]A. Rogach, S. V. Kershaw, M. Burt, M. T. Harrison, A. Kornowski, A. Eychmüller, and H. Weller, Adv. Mater. **11**, 552 (1999).
[6]M. T. Harrison, S. V. Kershaw, A. L. Rogach, A. Kornowski, A. Eychmüller, and H. Weller, Adv. Mater. **12**, 123 (2000).
[7]M. Kuno, K. A. Higginson, S. B. Qadri, M. Yousuf, S. H. Lee, B. L. Davis, and H. Mattoussi, J. Phys. Chem. B **107**, 5758 (2003).
[8]M. V. Kovalenko, E. Kaufmann, D. Pachinger, J. Roither, M. Huber, J. Stangl, G. Hesser, F. Schäffler, and W. Heiss, J. Am. Chem. Soc. **128**, 3516 (2006).
[9]A. Rogach, A. Eychmüller, S. Hickey, and S. Kershaw, Small **3**, 536 (2007).
[10]T. Rauch, M. Boberl, S. F. Tedde, J. Furst, M. V. Kovalenko, G. Hesser, U. Lemmer, W. Heiss, and O. Hayden, Nat. Photonics **3**, 332 (2009).
[11]S. Keuleyan, E. Lhuillier, and P. Guyot-Sionnest, J. Am. Chem. Soc. **133**, 16422 (2011).
[12]S. Kim, T. Kim, S. H. Im, S. I. Seok, K. W. Kim, S. Kim, and S.-W. Kim, J. Mater. Chem. **21**, 15232 (2011).
[13]S. Keuleyan, E. Lhuillier, V. Brajuskovic, and P. Guyot-Sionnest, Nat. Photonics **5**, 489 (2011).
[14]E. Lhuillier, S. Keuleyan, and P. Guyot-Sionnest, Nanotechnology **23**, 175705 (2012).
[15]H. Liu, S. Keuleyan, and P. Guyot-Sionnest, J. Phys. Chem. C **116**, 1344 (2012).
[16]X. W. Zhang and J. B. Xia, J. Phys. D: Appl. Phys. **39**, 1815 (2006).
[17]S. H. Groves, R. N. Brown, and C. R. Pidgeon, Phys. Rev. **161**, 779 (1967).
[18]P. Man and D. S. Pan, Phys. Rev. B **44**, 8745 (1991).
[19]J. P. Laurenti, J. Camassel, A. Bouhemadou, B. Toulouse, R. Legros, and A. Lusson, J. Appl. Phys. **67**, 6454 (1990).
[20]C.-Y. Moon and S.-H. Wei, Phys. Rev. B **74**, 045205 (2006).
[21]A. Svane, N. E. Christensen, M. Cardona, A. N. Chantis, M. van Schilfgaarde, and T. Kotani, Phys. Rev. B **84**, 205205 (2011).
[22]J. W. Nicklas and J. W. Wilkins, Phys. Rev. B **84**, 121308 (2011).
[23]R. Sakuma, C. Friedrich, T. Miyake, S. Blügel, and F. Aryasetiawan, Phys. Rev. B **84**, 085144 (2011).
[24]G. Bastard, Phys. Rev. B **25**, 7584 (1982).
[25]B. A. Bernevig, T. L. Hughes, and S.-C. Zhang, Science **314**, 1757 (2006).
[26]M. König, S. Wiedmann, C. Brüne, A. Roth, H. Buhmann, L. W. Molenkamp, X.-L. Qi, and S.-C. Zhang, Science **318**, 766 (2007).
[27]O. Madelung, M. Schultz, W. von der Osten, and U. Rössler, *Numerical Data and Functional Relationships in Science and Technology*, Vol. 22a (Springer-Verlag, Berlin, 1987).
[28]C. Delerue and M. Lannoo, *Nanostructures: Theory and Modeling* (Springer, New York, 2004).
[29]M. T. Czyżyk and M. Podgórny, Phys. Status Solidi B **98**, 507 (1980).
[30]K. C. Hass, H. Ehrenreich, and B. Velický, Phys. Rev. B **27**, 1088 (1983).
[31]J. N. Schulman and Y.-C. Chang, Phys. Rev. B **33**, 2594 (1986).
[32]M. Fornari, H. H. Chen, L. Fu, R. D. Graft, D. J. Lohrmann, S. Moroni, G. Pastori Parravicini, L. Resca, and M. A. Stroscio, Phys. Rev. B **55**, 16339 (1997).
[33]E. Martin, C. Delerue, G. Allan, and M. Lannoo, Phys. Rev. B **50**, 18258 (1994).
[34]A. Franceschetti, H. Fu, L. W. Wang, and A. Zunger, Phys. Rev. B **60**, 1819 (1999).
[35]G. Onida, L. Reining, and A. Rubio, Rev. Mod. Phys. **74**, 601 (2002).
[36]C. Delerue, M. Lannoo, and G. Allan, Phys. Rev. Lett. **84**, 2457 (2000).
[37]L. X. Benedict, Phys. Rev. B **66**, 193105 (2002).
[38]C. Delerue, M. Lannoo, and G. Allan, Phys. Rev. B **68**, 115411 (2003).
[39]D. Dexter, in *Solid State Physics*, Vol. 6, edited by F. Seitz and D. Turnbull (Academic Press, New York, 1958), p. 360.
[40]G. Allan and C. Delerue, Phys. Rev. B **70**, 245321 (2004).
[41]E. Groeneveld, C. Delerue, G. Allan, Y.-M. Niquet, and C. de Mello Donegá, J. Phys. Chem. C, doi:10.1021/jp3080942.
[42]J. C. Slater and G. F. Koster, Phys. Rev. **94**, 1498 (1954).
[43]Y. M. Niquet, C. Delerue, G. Allan, and M. Lannoo, Phys. Rev. B **62**, 5109 (2000).
[44]G. Allan, Y. M. Niquet, and C. Delerue, Appl. Phys. Lett. **77**, 639 (2000).
[45]P. Vogl, H. P. Hjalmarson, and J. D. Dow, J. Phys. Chem. Solids **44**, 365 (1983).
[46]J.-M. Jancu, R. Scholz, F. Beltram, and F. Bassani, Phys. Rev. B **57**, 6493 (1998).
[47]D. J. Chadi, Phys. Rev. B **16**, 790 (1977).
[48]T. B. Boykin, Phys. Rev. B **57**, 1620 (1998).
[49]F. J. Ohkawa and Y. Uemura, J. Phys. Soc. Jpn. **37**, 1325 (1974).